IMPROVED OBJECT RECOGNITION BY FUSION OF HYPERSPECTRAL AND SAR DATA

Dirk Borghys [1], Michal Shimoni [1], Gregory Degueldre [1] and Christiaan Perneel [2]

1. Royal Military Academy, Signal & Image Center, Brussels, Belgium, Dirk.Borghys@rma.ac.be
2. Royal Military Academy, Dept. of Applied Mathematics, Brussels, Belgium

ABSTRACT

The objective of the research presented in this paper is to investigate whether Polarimetric SAR (PolSAR) data can improve the classification results that are obtained from hyperspectral data in the case of highly complex scenes such as urban or industrial sites. Indeed SAR and hyperspectral sensors are sensitive to different characteristics of the imaged objects in the scene, i.e. hyperspectral provides information about surface material while SAR provides information about geometrical and dielectric properties of the objects. Combining both should thus allow to resolve classification ambiguities that exist when they are used separately.

In this paper supervised feature-based classification methods are used on the hyperspectral and SAR data separately and the results of these classifications are fused. The features used for the classification consist of the original bands for both sensors, the PCA bands for the hyperspectral data, the speckle reduced SAR data and results of various polarimetric decomposition methods from the POLSAR data. Two classification methods were used, a classical one and a newly developed one. The newly developed method is based on logistic regression (LR). LR is a supervised multi-variate statistical tool that finds an optimal combination of the input channels for distinguishing one class from all the others. The classical classification method is the matched filtering (MF). Both classification methods provide, besides a classification image, also probability images that give in each pixel the probability or abundance of a given class in that pixel. These can be used in the decision-level fusion. Three types of decision-level fusion are investigated: a weighted majority vote, a method based on Support Vector Machines (SVM) and one based on a binary decision tree.

The methods are applied on data of two urban areas in South of Germany that were acquired in Mai 2004. The collected data consists of HyMap (VIS-SWIR) and E-SAR data (L-band full-polarimetric and X-band HH- and VV-polarisation). The detected images included various man-made objects as residences, industrial buildings, forest, agriculture fields, airport and roads in rural-urban and industrial scenes. For calibration and verification ground truth data were collected using ASD spectrometer and digital topographic and cadastral maps of the areas were acquired.

An exhaustive comparison of the obtained classification and fusion results is performed. This comparison shows that fusion of PolSAR and hyperspectral data improves significantly urban object recognition.

INTRODUCTION

In urban and industrial areas, many man-made materials appear spectrally similar to moderate resolution optical sensors like Landsat TM. High spatial resolution sensor like IKONOS are also not sufficient to distinguish man-made objects constructed from different materials (i, ii, iii, iv). Some of man-made objects can be discriminated in a radar image based on their dielectric properties and surface roughness. For instance, building walls oriented orthogonal to the radar look direction form corner reflectors and have relatively strong signal returns. A smooth surface of bare soil, which acts as specular reflector, will result in relatively low signal returns. However, trees can introduce interpretation uncertainty by producing bright returns similar to buildings. Wet soil and other urban man-made features with high dielectric constants (e.g. vegetation, metal roofs) are confused in a radar image (v). Thus, there is no single sensor able to provide sufficient information to extract man-made object in the complex urban environment (vi). Instead, the way for increasing this analysis is the integration of features coming from different sources.

Classification of land cover is one of the primary objectives in the analysis of remotely sensed data. To aid in this process, data from multiple sensors are often utilised, since each potentially provides different information about the characteristics of the land cover. Thus, the fusion of multisensor data has received tremendous attention in the remote sensing literature (vii, viii, ix, x, xi) and mainly fusion of SAR with optical or thermal data (vi, xii, xiii, xiv, xv, xvi, xvii, xviii, xix, xx, xxi, xxii). Fusion of features extracted from polarimetric synthetic aperture radar and hyperspectral imagery was successfully conducted for land use mapping, urban characterisation and urban classification (xxiii,xxiv,xxv). However, those researches were devoted to detect built areas or to separate different soil use classes in urban areas, with no or little attention for single man-made objects or structures.

Over the next few years several EO satellites will be deployed in orbit, providing the international scientific, commercial and military communities with a wealth of new data. Many of these will carry advanced multi-channel imaging radars designed to combine various levels of polarisation diversity.

The main objective of this proposal is to resolve the classification ambiguity of several man-made objects in urban and industrial scenes using fused polarimetric SAR and hyperspectral data. Our main assumption is that while the polarimetric SAR measurements are sensitive to the surface geometry and the dielectric constant of the illuminated surface; hyperspectral data provide information related to the biochemical origin and environmental state of the observed area.

DATA SET

The data used in this paper were obtained in the frame of a project for the Belgian Federal Science policy. In May 2004 a flight campaign over Southern Germany was organised in order to acquire data from the Hymap sensor and the E-SAR sensor at the same time over urban and industrial sites. The data used in the illustrations in this paper are part of the scene acquired over the village of Neugilching.

Hyperspectral data

For this project HyMap data were acquired over the villages of Oberpfaffenhofen and Neugilching in the South of Germany. The HyMap data were acquired by the German Aerospace Agency DLR and contain 126 contiguous bands ranging from the visible region to the short wave infrared (SWIR) region (0.45–2.48μm). The bandwidth of each channel is 15-18 nm. The spatial resolution is 4 m at nadir and the complete image covers an area of 2.6×9.5 km. Four subsequent levels of pre-processing were applied: radiometric correction, geocoding, atmospheric correction (using ATCOR44) and the “Empirical Flat Field Optimized Reflectance Transformation” (EFFORT5). The pre-processing was done by the Flemish Institute for Technological Development (VITO). We received the data corresponding to the four different levels of pre-processing and for the moment only the last level is used. Later we intend to apply our methods to the different levels of preprocessed data in order to study the degradation of the classification results when less preprocessing steps are applied. One of the final aims of the project is to develop algorithms that require the least amount of pre-processing. In all processing the first and last channel were discarded. The first contains too much noise while the last is saturated.

SAR data

SAR data at 2 different frequencies were acquired by the E-SAR system of the German Aerospace Agency (DLR). L-band data (λ=23 cm) are full-polarimetric (HH- HV- and VV-polarisation were acquired). For X-band (λ =3 cm) only HH and VV polarisation were acquired. All data were delivered as Single-Look Complex (SLC) data as well as geocoded amplitude data. The DLR also provided geocoding matrices that enable one to extract polarimetric information using the SLC data and geocode the results afterwards. The spatial resolution of the geocoded SAR data is 1.5 m.

Figure 1: Left: Part of original Hymap image (in RGB color composite). Right: L-band polarimetric SAR image (R=HH,G=HV,B=VV)

Ground truth

For ground truthing of the acquired data, topograpic maps and cadaster maps of the area were obtained. Three levels of ground truth were defined: a learning set for the classification methods, a learning set for training the fuzzy-logic based fusion method and finally a validation set for evaluating the results of classification and fusion.

The considered classes are: “Roads”, “Buildings” (concrete roof), “Residence” (red roof buildings), “Buildings Grey” (grey roof buildings), “Grass”, “Bare soil” and “Parking lots”. The differences in types of buildings based on their roof type is necessary for the hyperspectral classification. For SAR classification on the other hand, these classes are merged into a single building class because the SAR sensor is not sensitive to the type of surface material.

SAR FEATURE EXTRACTION

From the available SAR data, different feature images were derived for classification. The first set consists of the speckle reduced amplitude data. These were determined from the geocoded data, for each channel separately. The second set consists of the results of various polarimetric decomposition methods. These were applied on the L-Band data in single-look complex data in slant-range coordinates and were geocoded later. For the polarimetric decompositions which require a spatial averaging using a sliding window, a 7x7 window was used.

Speckle Reduction

Standard speckle reduction methods tend to blur the image. In particular edges are smoothed and strong isolated scatterers are removed. Because these two features are very important, A. Pizurica developed a speckle reduction method based on context-based locally adaptive wavelet shrinkage (xxvi) and (xxvii). The idea is to estimate the statistical distributions of the wavelet coefficients representing mainly noise and representing useful edges. In particular it was noted that in SAR intensity images, the magnitudes of the wavelet coefficients representing mainly noise follow an exponential distribution while those representing a useful signal follow a Gamma distribution. This information is used to find a threshold that allows to distinguish useful signal from noise. Prior knowledge about possible edge configurations is introduced using a Markov Random Field.

Figure 2 shows the region of interest for the different available SAR images in RGB composition. The left image is the original L-band full-polarimetric image, the middle is the same image after speckle reduction and the right image is a combination of the different channels of the X- and L-band images after speckle reduction. The figure shows that the different polarisations and the two frequencies provide complementary information about the objects in the scene. Comparing the left and middle image shows that the speckle reduction is effective in reducing the speckle noise while preserving the detail in the image. This is particularly important in complex and highly heterogeneous scenes such as urban environments.

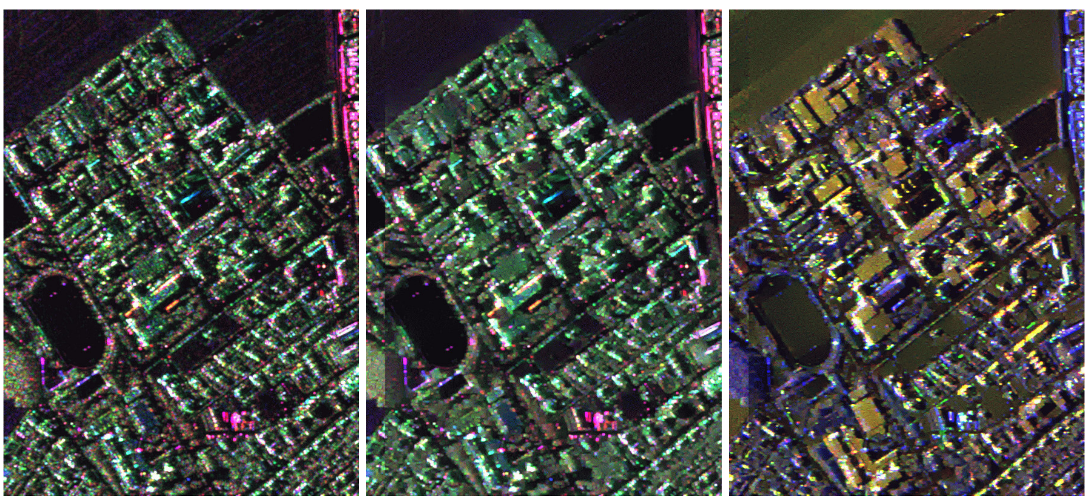

Figure 2: Available SAR images. Left: original SAR L-band image (R:HH,G:HV,B:VV), middle: same image after speckle reduction, right: combined speckle-reduced X- and L-band image (R:Xhh,G:Xvv,B:Lhh)

Polarimetric decompositions

For L-band full-polarimetric data were acquired. This means that in every pixel of the image, the complete scattering matrix was measured. The scattering matrix describes the complete polarimetric signature of the points on the ground. This polarimetric signature depends on the type of scattering induced by these objects on the ground on the incoming radar wave. Polarimetric decomposition methods combine the polarimetric information in a way that allows inferring information about the type of scattering produced by the elements on the ground on the radar waves.

Several decomposition methods were developed in the past; each of them highlighting specific types of scattering behaviour. The most well known method is the Cloude & Pottier (xxviii) decomposition. Several parameters were derived from their method: entropy H, scattering angle

α, combinations of the entropy and anisotropy A: HA, H(1-A), (1-H)A and (1-H)(1-A) and the value of the largest eigenvalue of the polarimetric coherency matrix, $\lambda 1$.

The other decomposition methods convert the polarimetric information into an abundance of three types of scattering. In this paper the decomposition methods of Barnes and Holm (xxix), Huynen (xxx), Freeman (xxxi) and Krogager (xxxii) are also considered. Figure 3 shows the results of the various decomposition methods. The figure shows that the different decomposition methods highlight different aspects of the scene. On the other hand the fact that they need to be determined using averaging windows on the slant-range image (7x7 in this case), introduces artefacts and reduces the resolution of the results. Whereas it was already show (xxxiii) that these features are very important for classifying agricultural scenes, they are likely to be less valuable in urban scenes where it is very important to keep the highest possible spatial resolution.

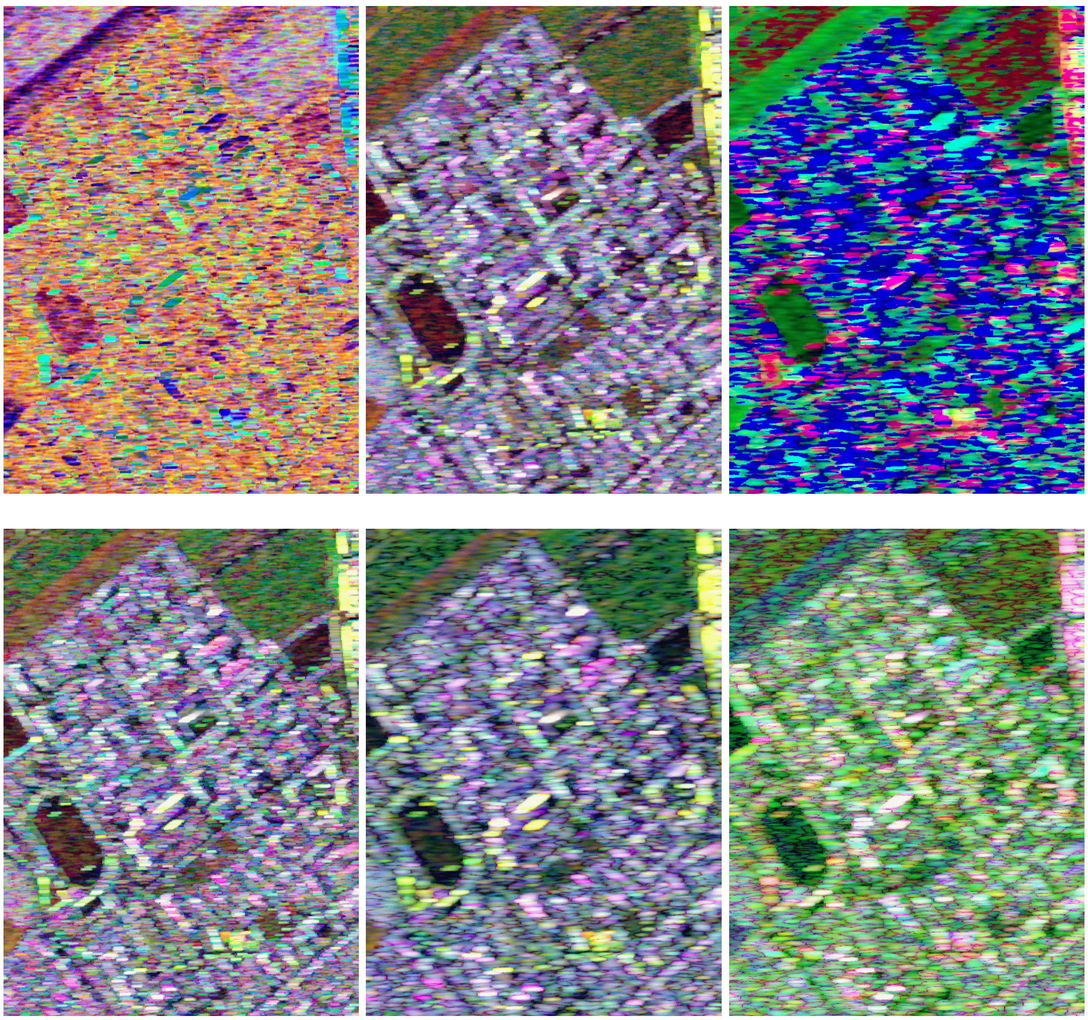

Figure 3: Results of the applied polarimetric decompositions Cloude (H,α,A), Barnes, Freeman, Holm, Huynen and Krogager.

DETECTION AND CLASSIFICATION METHODS

For this project on fusion we have chosen to use classification methods that are based on a detection per class in each pixel. The first method does this by assigning abundances of each class to each pixel. The second method provides probability images for each class. These can be combined into a classification image by assigning to each pixel the class for which respectively the abundance or probability is highest. However the advantage of using classifiers based on detectors that provide probabilities is that it is also possible to delay the decision until the results of different classifications or input feature sets are fused. This will be used in two of the developed decision-level fusion methods discussed in below.

Matched filter

The matched filter (xxxiv) detects the abundance of end-members in each pixel of the hyperspectral image by matching their spectrum to the one of each end-member or to the average of the spectra of each class of the learning set. The result is an abundance measure for each class that in each pixel estimates the proportion of that class within the pixel. This is a “soft classification”. In order to obtain a pixel-wise classification image, to each pixel the class corresponding to the highest abundance is assigned. This results in a “hard classification”. As mentioned before, for fusion, either the soft or the hard classification results can be combined.

Detection and classification using logistic regression

Logistic regression (LR) (xxxv) is developed for dichotomous problems where a target class has to be distinguished from the background. The method combines the input parameters into a non-linear function, the logistic function:

$$p_{x,y}\left(\text{target} \mid \vec{\mathrm{C}}\right)=\frac{\exp\left[\beta_0+\sum_i F_i(x,y)\beta_i\right]}{1+\exp\left[\beta_0+\sum_i F_i(x,y)\beta_i\right]}$$

$p_{x,y}\left(\text{target} \mid \vec{F}\right)$ is the conditional probability that a pixel (x,y) belongs to the considered class (target class) given the vector of input features $\vec{F}$ at the given pixel. $F_i(x,y)$ is the value of pixel (x,y) in the i^{th} feature.

The logistic regression (i.e. the search for the weights β_i) is carried out using Wald's forward stepwise method using the commercial statistics software SPSS. In the Wald method, at each step, the most discriminating feature is added and the significance of adding it to the model is verified. This means that only the features that contribute significantly to the discrimination between the foreground and the background class are added to the model. The LR thus implicitly performs a feature selection.

Applying the obtained logistic function for a given target class to the complete image set, a new image - a ``detection image'' - is obtained, in which the pixel value is proportional to the conditional probability that the pixel belongs to the target class, given the set of used features.

The detection images for the different classes are combined into a classification image by attributing to each pixel of the classification image the class that corresponds to the highest value of the detection image.

DECISION-LEVEL FUSION

Three decision-level fusion methods were used and compared in this paper. They are briefly described below.

Weighted majority vote

The confusion matrices obtained from the intermediate learning set were used to design a weighted majority vote. The method uses the probability or abundance images for each class as given by the LR-based and the MF-based classifiers respectively.

In a first step the probabilities for each class from the different classifiers are summed using a weighted sum. The weights of the sum are determined using the average of the UA and PA for the class with respect to the sum of theses averages over the different classifications to be fused.

$$P_i(x,y) = \sum_{j=1}^{Nclassifiers} w_{ij} P_{ij}(x,y)$$

where

$$w_{ij} = \frac{UA_j + PA_j}{\sum_{k=1}^{Nclassifiers} \left(UA_k + PA_k\right)}$$

Pi(x,y) is the probability of having class i in pixel (x,y) averaged over all classifiers, Pij(x,y) is the probability for detector (or classifier j).

The class i for which Pi is largest, is assigned to the pixel.

SVM based fusion

A support vector machine (xxxvi) using radial basis functions was used to combine the probability images from the different classifiers. The SVM of the commercial software package ENVI was used.

Decision tree based fusion

A simple binary decision tree classifier (xxxvi) was used to combine the different classification images. The decision tree implements simple rules such as:

Assign (x,y) to Resid if (C1(x,y)=Resid and ((C2(x,y)=Resid) or (C3(x,y)=AnyBuilding))

For this paper the binary decision tree implemented in ENVI was used.

RESULTS

Classification results

Different classification results were compared:

- Results of matched filtering applied on the 30 first PCA channels obtained from the HyMap data (MF PCA 1-30)
- Results of logistic regression from the 124 original HyMap channels (LR_optical). This is possible because the LR performs an implicit channel selection.
- Results of LR on original SAR data and speckle reduced SAR data (LR OrigSAR & SR)
- Results of LR on polarimetric decomposition images (LR Polsar)
- Results of LR of the combined SAR set (LR ALLSAR)

Table 1 shows the user accuracy and producer accuracy for each of the classification results. From the table it is clear that the two classifications based on the HyMap data give better results than those obtained from the SAR data. Furthermore the results of LR on the original HyMap channels are better than those obtained by the Matched filter on the PCA bands.

While the SAR results are less good than the hyperspectral results, the difference between them is not that large for some of the classes. Furthermore detailed examination of the confusion matrices show that different combinations of classes are confused in the SAR classification than in the hyperspectral classification. This is the reason why fusion is likely to improve the classification results.

Table 1: Classification results for hyperspectral data

Classes	Hyperspectral			
	MF PCA1-30		LR Optical	
	PA %	UA %	PA %	UA %
Roads	94.81	81.56	95.78	44.7
Buildings	51.66	85.93	78.55	100
Residence	98.33	88.94	100	100
BuildingGrey	100	71.58	98.49	100
Bare Soil	100	99.31	100	100
Parking Lots	63.42	65.75	94.1	80.76
Grass	95.38	99.37	87.17	99.65

Table 2: Classification results for SAR data

Classes	SAR					
	LR OrigSAR & SR		LR POLSAR		LR ALLSAR	
	PA %	UA %	PA %	UA %	PA %	UA %
Roads	38.31	30.73	27.27	23.86	63.31	24.38
Buildings						
Residence	75.57	83.13	79.89	80.56	77.59	89.61
BuildingGrey						
Bare Soil	95.47	65.39	91.81	63.96	97.39	70.49
Parking Lots	99.12	57.93	83.78	18.65	91.15	36.4
Grass	80.62	98.61	42.92	96.68	57.87	97.57

Visual comparison of detection results

Both the matched filter and the logistic regression result in detection or rule images for each class that represent in each pixel the probability of that pixel belonging to the considered class. It is interesting to examine these detection images for each class for the different classifications that were used. Figure 4 show on the left a color composite of three detection images corresponding to the class “residential”, i.e. red-roofed buildings. In red is the result of the logistic regression based using the HyMap data, green: results of matched filtering, blue is the detection result of all buildings obtained by LR on the complete set of SAR feature images. For most true red-roofed buildings the three classifiers agree (white on the left image). However, there are three regions that only the first classifier detects as residential. On the color composite HyMap image they indeed seem red, On the SAR image on the other hand they are very dark; corresponding to a smooth area. The region on the left of the image is the running piste and the athletic facilities of a sport stadium, the one just below is a parking area and the rectangular region on the upper right is actually a tennis court (as verified by the cadaster map). From this visual inspection it is clear that the fusion can indeed improve the classification results in highly complex scenes such as urban or industrial sites. It is easy to highlight these differences between classifications automatically. Interpreting them correctly is quite a different matter and requires skilled photo-interpreters. Nevertheless, a set of images as shown in Figure 4 could greatly facilitate the work of manual photo-interpretation.

Figure 4: Left: Fused detection result for the class "residential", middle: corresponding Hymap image. Right: SAR composite (R=Xhh, G=Xvv, B=Lhh)

Decision-level fusion results

Table 3 shows the UA and PA for the different classes that were obtained by the various decision-level fusion methods. The fusion was performed by combining four results: the results of the MF on the 30 first PCA bands, the LR on all Hymap bands, the LR on the combined set of original and speckle reduced SAR data and the LR results of the POLSAR decompositions. For the weighted majority vote and the SVM the probability (or abundance) images were used as input. For the decision tree fusion, the classification images were used. All fusion methods use a second training set that is independent of the training set used for training the classifiers and also independent of the validation set that was used to construct the confusion matrices.

The table shows that all types of fusion do indeed improve the classification results when compared to the UA and PA presented in Table 1 and Table 2. The decision tree gives the best results. Figure 5 shows the results of the three decision-level fusion methods. For the decision tree fusion a class “unclassified” is present because not all possible nodes of the tree are assigned to a class. These unclassified areas should be examined further.

Table 3: Results of the different decision-level fusion methods

Classes	Fusion Results					
	Weighted Maj. Vote		SVM		Decision Tree	
	PA %	UA %	PA %	UA %	PA %	UA %
Road	99.07	42.8	100	32.6	99.65	83.09
Building	59.37	77.15	81.56	100	76.05	100
Residence	91.12	98.87	100	100	100	90.24
BuildGrey	100	100	100	100	100	100
Bare Soil	100	93.44	100	100	100	100
Parking Lots	94.29	95.66	92.37	98.09	98.09	99.83
Grass	42.64	100	34.05	100	100	100

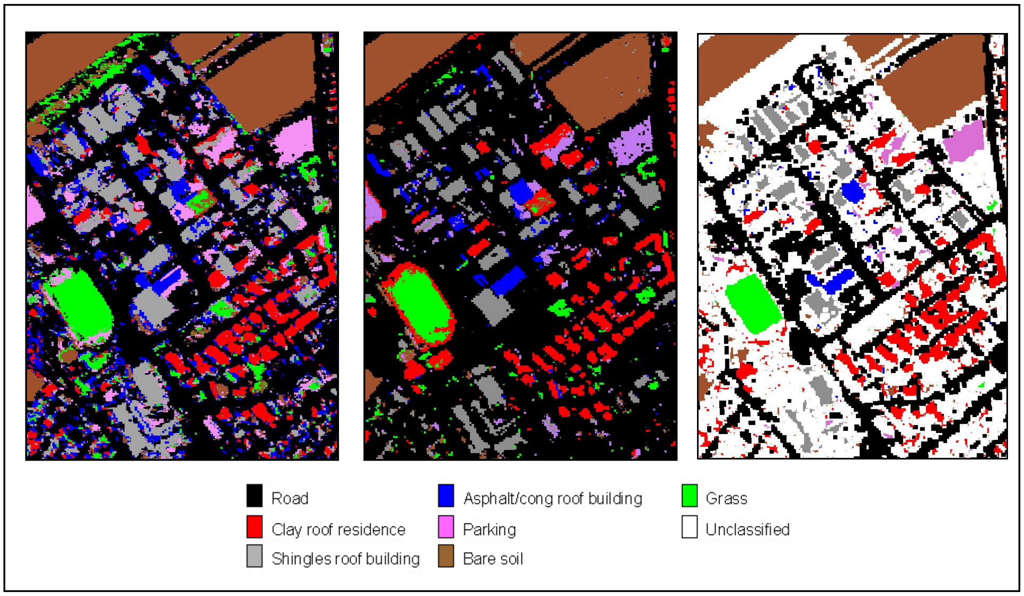

Figure 5: Result of the decision-level fusion. Left: Majority Vote, middle: SVM, right: Decision Tree

CONCLUSIONS

This paper investigates the fusion of hyperspectral and polarimetric SAR (PolSAR) data for the classification of urban scenes. The first step in the processing consist in feature extraction and feature-based supervised classification. Classification results are fused at the decision level. Three types of decision-level fusion are used and results compared.

Two classifiers were applied: the matched filter and a classifier based on logistic regression. Both provide, besides a classification image, abundance or probability images for each class that can be used for the fusion.

The comparison of classification results obtained from SAR and hyperspectral show that, when used as single sensors, the hyperspectral outperforms the SAR. However the SAR results are still of good quality and furthermore the confused classes are different for SAR and hyperspectral. This is a first indication that their fusion could improve the results.

Three fusion methods were applied in the frame of this paper: a weighted majority vote, a support vector machine and a decision tree They all combine the classification or detection results. The results of fusion are better than those obtained for a single sensor. This shows that the two types of sensors are indeed complementary. The best results are obtained for the decsion tree based fusion, for which a global kappa of 98% is reached on the validation set. These results need to be verified further on larger regions and different test-sites.

The main added value from the SAR comes from the speckle reduced images. It was noted in this research that the results of polarimetric decomposition of the PolSAR do not add significantly to the classificationresult for urban areas, contrary to agricultural areas where it is very important. The reason for this is that the polarimetric decomposition is calculated on running averaging windows (of 7x7) and this degrades the spatial resolution. A possible solution could be to segmet the image first and calculate the decompositions only inside the uniform regions. This is a topic for further research.

On the other hand we would like to investigate spatial reasoning and the effect of adding the results of a dark and bright line detector in the SAR feature set. Other types of decision fusion e.g. fuzzy-logic based fusion or methods based on dempster-shafer or neural networks will also be investigated.

ACKNOWLEDGMENTS

The data for this project were acquired through a collaboration with the German Aerospace Agency DLR, the Flemish Institute for Technological development (VITO) and RMA in the frame of a project "HySAR" funded by the Belgian Federal Science Policy. The speckle reduction algorithm was kindly provided to us by Dr A. Pizurica of Ghent University.

REFERENCES

i 1. B. C., Forster, "An examination of some problems and solutions in monitoring urban areas from satellite platform", International Journal of remote Sensing, 6 (1), 139-151, 1985.

ii G. F. Hepner, Houshmand, B., Kulikov, I. and Bryant, N., "Investigation of the integration of AVIRIS and IFSAR for urban analysis", Photogrammetric Engineering and Remote Sensing, 64 (8), 813-820, 1998.

iii C. M., Chen, Hepner, G. F. and Forster, R. R., "Fusion of hyperspctral and radar data using the HIS transformation to enhance urban surface features", Photogrammetric Engineering and Remote Sensing, 58, 19-30, 2003.

iv C., Small, "Global Analysis of Urban Reflectance", International Journal of Remote Sensing, 2004.

v F. M., Henderson and Xia, Z. G., "SAR application in human settlement detection popula-tion estimation and urban land use pattern analysis: a sttus report", IEEE Transaction on Geosciences and Remote Sensing, 35, 79-85, 1997.

vi P. Gamba and Houshmand, B., "Urban remote sensing through multispectral and radar data", Proceeding of the ERS/ENVISAT symposium, Gothenbourg'2000, 272-278, 2000.

vii P. S., Chaves, Sides, S. C., and Anderson, J. A., "Comparison of three different methods to merge multiresolution and multispectral data: Landsat TM and SPOT panchromatic", Photogrammetric Engineering and Remote Sensing, 57 (3), 295-303, 1991.

viii K. O., Niemann, Goodenough, D. G., Marceau, D. and Hay, G., "A practical alternative for fusion of hyperspectral data with high resolution imagery", Proceeding of IGARSS'98, I, 174-176, 1998.

ix P. Gamba and Houshmand, B, "Three-dimentional road network by fusion of polarimetric and interferometric SAR data", Proceeding of IGARSS'99 I, 302-304, 1999.

x K. Saraf, "IRS-1C-LISS-III and Pan data fusion: an approach to improve remote sensing based mapping techniques", International Journal of remote Sensing, 20 (10), 1929-1934, 1999.

xi Y, Zhang, "A new merging method and its spectral and spatial effects", International Journal of remote Sensing, 20 (10), 2003-2014, 1999.

xii S. S. Yao and Gilbert, J. R., "Registration of synthetic aperture radar image to thematic mapper imagery for remote sensing applications", IEEE Trans. on Geosciences and remote Sensing, GE-22 (6), 557-563, 1984.

xiii D. J. Weydahl, Becquery, X. and Tollefsen, T, "Combining ERS-1 SAR with optical satellite data over urban area, Proceeding of IGARSS'1995, 3, 2161-2163, 1995.

xiv K. S., Kierein-Young, "Integration of optical and radar data to characterize mineralogy and morphology of surfaces in Death Valley, California", International Journal of Remote Sensing, 18 (7), 1517 – 1541, 1997.

xv R. Welche and Ehler, M., "Cartographic feature extraction with integrated SIR-B and Land-sat TM images", International Journal of remote Sensing, 9 (5), 873-889, 1998.

xvi N. Milisavljevic, Bloch, I. and Acheroy M., "Characterisation of mine detection sensors in terms of belief functions and their fusion, first results", In: Proc. 3rd Int. Conference on information fusion, WeD3-24, 2000.

xvii L. Fatone, Maponi, P. and Zirilli, F., "Fusion of SAR/optical images to detect urban areas", IEEE/ISPRS joint workshop'2001 on remote sensing and data fusion over urban area, 217-221, 2001.

xviii B. A. Lofy and Sklansky, J., "Segmenting multisensor aerial images in class-scale space", Pattern recognition, 34, 1825-1839, 2001.

xix I., Sandholt, "The combination of polarimeric SAR with satellite SAR and optical data for classification of agriculture land", Danish Journal of Geography, 101, 21-32, 2001.

xx O., Hellwich, Reigber, A. and Lehmann, H, "Sensor and data fusion context: test imagery to conduct and combine airborne SAR and optical sensors for mapping", Proceeding of IGARSS'2002, 1, 82-84, 2002.

xxi M., Pellizzeri, Oliver, C. J., Lombardo, P. and Bucciarelli, T., "Improved classification of SAR images by segmentation and fusion with optical images", Proceeding of Radar'2002, 158-161, 2002.

xxii R. N., Treuhaft, Asner , G. P. and Law, B. E., "Forest Biomass Based on Leaf Area Densi-ties from Multialtitude AIRSAR Interferometry and AVIRIS Spectroscopy", AirSAR'2002 Workshop JPL, 2002.

xxiii G. F., Hepner, Houshmand, B., Kulikov, I. and Bryant, N., "Investigation of the potential for the integraton of AVIRIS and IFSAR for urban analysis", Photogrammetric Engineering and Remote Sensing, 64 (8), 512-520, 1998.

xxiv P. Gamba and Houshmand, B., "Hyperspectral and IFSAR for 3D urban characterisation", Photogrammteric engineering and remote sensing, 67, 944-956, 2000.

xxv Y., Allard, Jouan, A. and Allen, S., "Land Use Mapping using Evidential Fusion of Polarimetric Synthetic Aperture Radar and Hyperspectral Imagery", Information fusion, 2005.

xxvi Pizurica A, W Philips, I Lemahieu & M Acheroy, 2001. Despeckling SAR images using wave-lets and a new class of adaptive shrinkage estimators, In: Proceedings IEEE 2001 Confe-rence on Image Processing, 2: 233-236 xxvii A. Pizurica, Image denoising using wavelets and spatial context modelling, PhD Thesis, University of Ghent, Faculty of Applied Sciences, Dept. of Telecommunications and Information Processing, June 2002.

xxviii Cloude S. R. and Pottier E., 1997. An entropy based classification scheme for land applications of polarimetric SAR. IEEE Trans. on Geoscience and Remote Sensing, 35: 68-78

xxix Holm and Barnes 1988. On radar polarization mixed target state decomposition techniques In: Proc. IEEE Radar Conference, Ann Arbor, MI, USA, pp 249-254

xxx Huynen 1970, Phenomenological theory of radar targets, PhD thesis, University of Technology, Delft, The Netherlands

xxxi Freeman A. and Durden S.L., 1997, A three-component scattering model for polarimetric SAR data, IEEE Trans. on Geoscience and Remote Sensing, vol. 36, nr. 1, pp 68-78

xxxii Krogager 1993. Aspects of polarimetric radar imaging, PhD Thesis, Tech. Univ. of Denmark.

xxxiii M. Shimoni, D. Borghys, N. Milisavljevic, C. Perneel, D. Derauw, and A. Orban. Feature recognition by fusion of polinsar and optical data. In Proc. ESA PolInSAR'07 Workshop, Rome, Italy, January 2007.

xxxiv Funk C.C., Theiler J., Roberts D.A. and Borel C.C., Clustering to improve matched filter detection of weak gas plumes in Hyperspectral Thermal Imagery", IEEE Trans. on Geoscience and Remote Sensing, 39(7), July 2001.

xxxv Hosmer D., Lemeshow S. 2000, Applied Logistic Regression (2nd Ed.)., Wiley & Sons

xxxvi Duda R.O., Hart P.E. and Stork D.G., Pattern Classification 2nd ed., Wiley Interscience, 2000